

Design, Synthesis, and Biological Evaluation of some methyl 2-(1*H*-pyrazol-4-ylthio)-1,2,3,4-tetrahydro-6-methylpyrimidine-5-carboxylate derivatives as potential DHFR inhibitors

Pathan Sherkh Khan Yusufkhan^{a,b*}, Suparna R. Deshmukh^c, Mazahar Farooqui^d

^aDepartment of Chemistry, Dr. Rafiq Zakaria College for Women, Aurangabad, Maharashtra 431001, India.

^bDepartment of Chemistry, Kohinoor Arts, Commerce and Science College Khultabad, Aurangabad, Maharashtra 431001, India.

^cDepartment of Chemistry, S. K. Gandhi College, Kada, Tal: Ashti, Dist: Beed, Maharashtra 414202, India.

^dDepartment of Chemistry, Maulana Azad College of Arts, Science and Commerce, Aurangabad 431004, India.

*Corresponding author email: sherkhkhanpathan01.91@gmail.com

Received: 28 Nov 2021

Revised: 10 Dec 2021

Accepted & Published: 23 Dec 2021

Abstract

Drug-resistant bacteria pose an increasingly serious threat to mankind all over the world. However, the currently available clinical treatments do not meet the urgent demand. Therefore, it is desirable to find new targets and inhibitors to overcome the problems of antibiotic resistance. Dihydrofolate reductase (DHFR) is an important enzyme required to maintain bacterial growth, and hence inhibitors of DHFR have been proven as effective agents for treating bacterial infections. In the present work, we have designed some methyl 2-(1*H*-pyrazol-4-ylthio)-1,2,3,4-tetrahydro-6-methylpyrimidine-5-carboxylate derivatives as potential DHFR inhibitors through rational drug design approach. The designed derivatives were screened through Lipinski rule, Veber's rule, ADMET analysis, drug-likeness properties, and molecular docking. All the compounds demonstrated more potent activity than Ampicillin against both gram-positive and gram-negative bacteria. Most of the compounds were more or equipotent than Chloramphenicol and Ciprofloxacin. Compound **B6** was sensitive at 50 µg/mL against all the bacteria. Compound **B16** was sensitive at 25 µg/mL against *Escherichia coli*, 50 µg/mL against *Pseudomonas aeruginosa*, and *Staphylococcus aureus* whereas compound **B20** was sensitive to all gram +ve and -ve bacteria at same concentration. In antifungal activity, compound **B7** exhibited MFCs of 100 µg/mL against *Candida albicans*, *Aspergillus niger*, and *Aspergillus clavatus* which is same

as Nystatin. Compound **B16** and **B20** were also sensitive to all the antifungal strains at 100 or 200 µg/mL concentration. Compound **B20** is more potent than Greseofulvin against *Candida albicans*. We concluded that compounds **B6**, **B7**, **B16** and **B20** are most potent and can developed further to get more promising molecules for the treatment of bacterial infection.

Keywords:DHFR, Biginelli reaction, Pyrimidines, Antibacterial, Molecular docking

1. Introduction

One of the most serious risks to public health today is the emergence of germs that are resistant to the majority of the common treatment medications(Murali et al., 2014; Sánchez-Sánchez et al., 2017). Drug-resistant bacteria, such as methicillin-resistant *Staphylococcus aureus* (MRSA) and multidrug-resistant *Escherichia coli*, cause great difficulties in the treatment of nosocomial infections, which severely threaten global public health(Anwar et al., 2020; Jouhar et al., 2020; Loi et al., 2019).According to a UK Government analysis, "the cost in terms of lost global productivity between now and 2050 will be an astonishing 100 trillion USD if we do not take action". Fungal infections can represent a major hazard to human health, particularly in immunocompromised people. Invasive fungal infections (IFIs) provide a huge worldwide problem in terms of clinical management(Indora and Kaushik, 2015; Marchese et al., 2016; Rahman et al., 2009). As a result, the need for novel antimicrobial agents that are distinct from current agents is emphasized.

The dihydrofolate reductase (DHFR) enzyme has been shown to be a therapeutic target for treating infections since the mid-20th century. In both prokaryotic and eukaryotic cells, DHFR is involved in the creation of raw material for cell proliferation by catalyzing the reduction of dihydrofolate to tetrahydrofolate utilizing NADPH. DHFR inhibitors are frequently used to treat fungal, bacterial, and mycobacterial diseases, as well as to combat malaria. Various compounds and medications have been developed and introduced to the market throughout the years(He et al., 2020; Songsunthong et al., 2021; Wróbel et al., 2020).

Compounds based on the pyrimidine scaffold are known to exhibit many different biological actions such as antibacterial, antifungal, anti-inflammatory and antitumor activities(Mittersteiner et al., 2021; Nerkar, 2021; Verma et al., 2020). Lots of amino pyrimidine-based derivatives have been reported to exhibit antibacterial activities via inhibiting

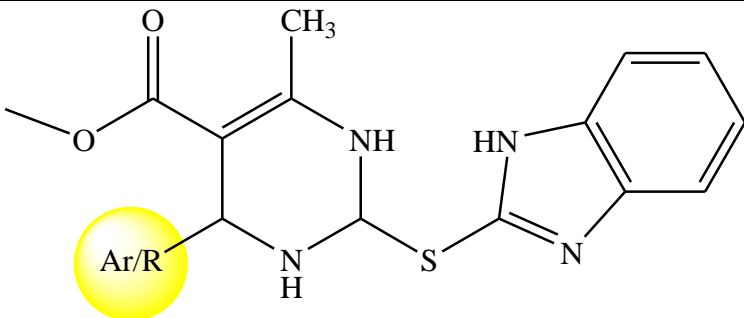
DHFR(Ahmed Elkanzi, 2020; Bhat et al., 2017). Therefore, in present study we have selected pyrimidine scaffold to design and develop some DHFR inhibitors as potential antibacterial and antifungal agents. The designed derivatives were first screened through ADMET property calculations and then those possess drug-likeness properties were subjected for molecular docking studies. The derivatives which found significant DHFR inhibition potential were subjected for wet lab synthesis followed by spectral analysis and biological evaluation.

2. Material and Methods

Designing of Derivatives

In the present work, we have designed some methyl 2-(1*H*-pyrazol-4-ylthio)-1,2,3,4-tetrahydro-6-methylpyrimidine-5-carboxylate derivatives as illustrated in Table 1. After designing of derivatives, all the molecules were subjected for in silico screening to check drug-likeness properties.

Table 1. The designing approach of methyl 2-(1*H*-pyrazol-4-ylthio)-1,2,3,4-tetrahydro-6-methylpyrimidine-5-carboxylate derivatives

 <p>methyl 2-(1<i>H</i>-benzo[<i>d</i>]imidazol-2-ylthio)-1,2,3,4-tetrahydro-6-methylpyrimidine-5-carboxylate</p>			
Compound code	Ar/R	Compound code	Ar/R
B1	—H	B11	—3-hydroxy phenyl
B2	—phenyl	B12	—2,3,4-trihydroxy phenyl
B3	—4-nitro phenyl	B13	—3-methoxy-4-hydroxy phenyl
B4	—4-bromo phenyl	B14	—2-methoxy phenyl
B5	—4-fluoro phenyl	B15	—4-styryl
B6	—4-chloro phenyl	B16	—naphthyl
B7	—4-methyl phenyl	B17	—2,4-dinitro phenyl
B8	—4-methoxy phenyl	B18	—4-methylsulfonyl phenyl
B9	—4-hydroxy phenyl	B19	—4-dimethylamino phenyl
B10	—3-nitro phenyl	B20	—4-trifluoromethyl phenyl

Pharmacokinetics and toxicity predictions of designed derivatives

Utilizing molinspiration and SwissADME servers, Lipinski rule of five and pharmacokinetic features of developed derivatives were investigated (Kim et al., 2021) (Daina et al., 2017). An *in silico* toxicity prediction of designed derivatives has been made using ProTox-II, a webserver that is freely available (http://tox.charite.de/protox_II) (Banerjee et al., 2018).

Molecular Docking

After screening through *in silico* ADMET analysis, the screened molecules were subjected for the molecular docking studies. The proposed derivatives and the native ligand were docked against the crystal structure of the wild-type *E.coli* dihydrofolate reductase using Autodockvina 1.1.2 in PyRx 0.8 (Dallakyan and Olson, 2015). ChemDraw Ultra 8.0 was used to draw the structures of the intended derivatives and native ligand (mole. File format). All the ligands were subjected for energy minimization by applying Universal Force Field (UFF) (Rappé et al., 1992). RCSB Protein Data Bank (PDB) entry 5CCC contains the wild-type *E.coli* dihydrofolate reductase complexed with 5,10-dideazatetrahydrofolate and oxidized nicotinamide adenine dinucleotide phosphate (<https://www.rcsb.org/structure/5CCC>). Discovery Studio Visualizer (version-19.1.0.18287) was used to refine the enzyme structure, purify it, and get it ready for docking (San Diego: Accelrys Software Inc., 2012). A three-dimensional grid box (size_x=39.7765672935 Å; size_y=40.0725575009 Å; size_z=35.1695000152 Å) with an exhaustiveness value of 8 was created for molecular docking (Dallakyan and Olson, 2015). BIOVIA Discovery Studio Visualizer was used to locate the protein's active amino acid residues. The approach outlined by Khan et al. was used to perform the entire molecular docking procedure, identify cavity and active amino acid residues (Chaudhari et al., 2020; S. L. Khan et al., 2021; S.L. Khan et al., 2020; Sharuk L. Khan et al., 2020; Siddiqui et al., 2021). Fig. 1 shows the revealed cavity of DHFR with the co-crystallize ligand molecule.

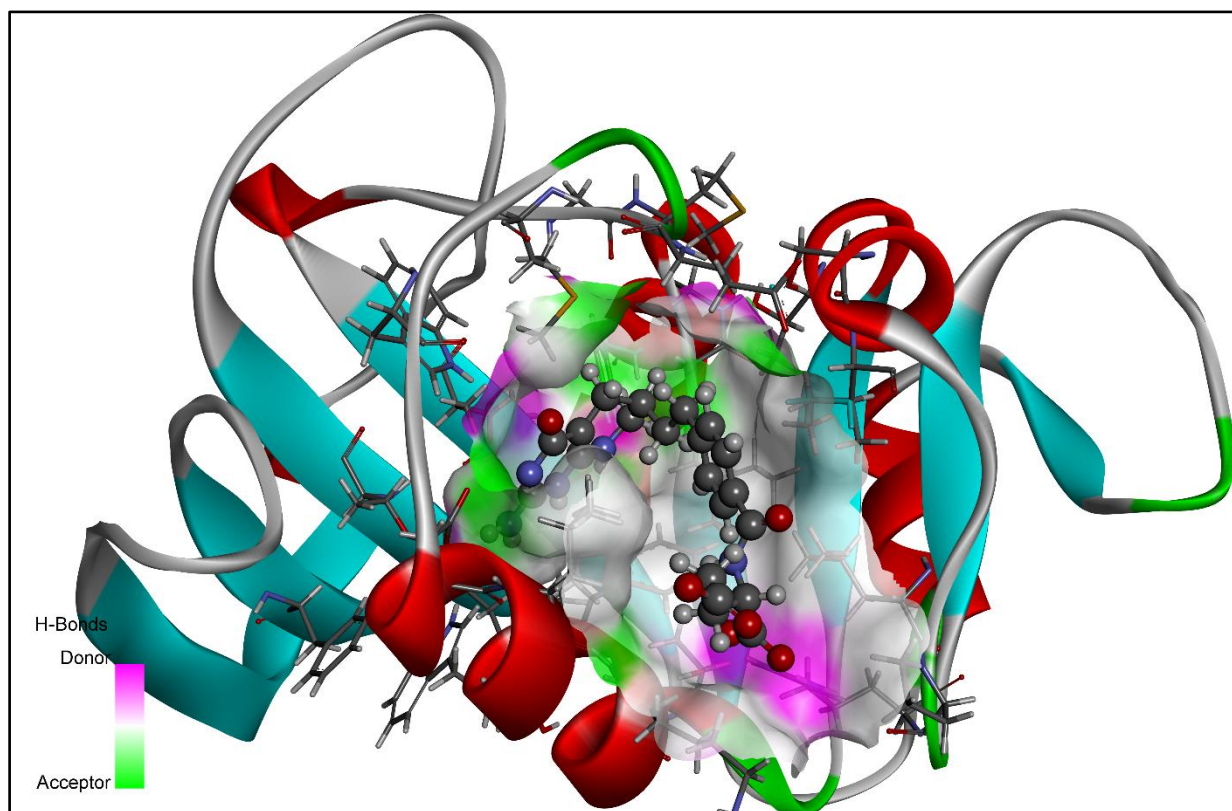


Fig.1. 3D ribbon view of DHFR with native ligand in allosteric site

Reaction Scheme and Synthesis of selected derivatives

From *in silico* screening and molecular docking studies, compounds **B6**, **B7**, **B16**, **B17** and **B20** were selected for the synthesis. All the required chemicals i.e. ethyl acetoacetate, aldehyde, thiourea, ferric chloride ($\text{FeCl}_3 \cdot 6\text{H}_2\text{O}$), conc. HCl, ethanol, 4-chloropyrazole, potassium hydroxide (KOH), and acetone of synthetic grade were purchased and procured from Lab Trading Laboratory, Aurangabad, Maharashtra, India. The progress of the reaction was confirmed by Thin-layer chromatography [TLC, (Merck precoated silica GF 254)] and compounds were subjected for spectral analysis by ^1H , ^{13}C NMR (on a Varian-VXR-300S at 400 MHz NMR spectrometer) and Mass spectroscopy with chloroform (d_6) as the solvent and TMS as the internal standard; chemical shift values were expressed in δ ppm. The melting points were measured using the VEEGO MODEL VMP-D melting point apparatus. The detailed procedure for the synthesis of derivatives is discussed in the below section.

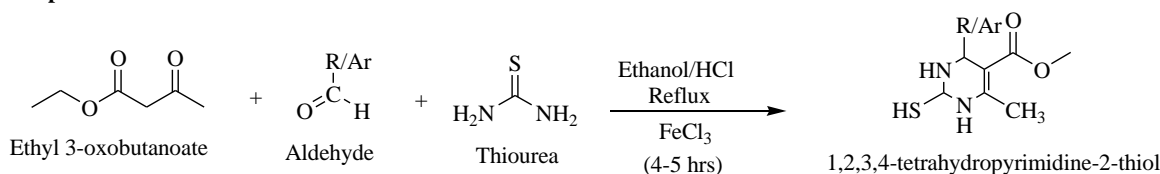
Step-I: Synthesis of 1,2,3,4-tetrahydropyrimidine-2-thiol

The reaction is a modified Biginelli reaction that generates 1,2,3,4-tetrahydropyrimidine-2-thiol from ethyl acetoacetate, aldehyde and thiourea^[3,4]. A solution of ethyl acetoacetate (1.3gm, 10 mmol), thiourea (1.14gm, 15 mmol), ferric chloride ($\text{FeCl}_3 \cdot 6\text{H}_2\text{O}$, 2.5 mmol) and conc. HCl (1-2 drops) in EtOH (20 mL) was heated independently with appropriate aldehydes (10 mmol), under reflux for 4-5 hrs^[5]. After cooling, the reaction mixtures were poured onto crushed ice (100gm). Stirring was continued for several minutes, the solid products were filtered, independently washed with cold H_2O (2 times 50 mL) and a mixture of EtOH- H_2O , 1:1 (3 times 20 mL). The solids were dried and recrystallized from hot EtOH to afford pure products. The m.p. was recorded and is uncorrected. The yields obtained were in the range of 75-95%.

Step-II: Synthesis of final pyrimidine derivatives

4-chloropyrazole (1.66 gm, 0.01 mol.) and 1,2,3,4-tetrahydropyrimidine-2-thiols (0.01 mol.) were condensed by heating with Potassium hydroxide (KOH) and H_2O : Acetone (2:1) at about 50-60°C for 45 min. Then the reaction mixture cooled to room temperature and then poured into ice-cold water, the precipitate was separated by filtration and recrystallized from ethanol. The yield was 90-95%.

Step-I:



Step-II:

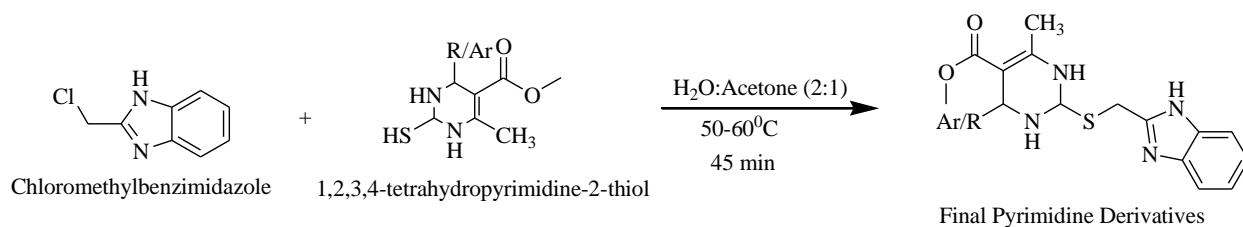


Fig. 2. The proposed reaction scheme for the synthesis of methyl 2-(1H-pyrazol-4-ylthio)-1, 2, 3, 4-tetrahydro-6-methylpyrimidine-5-carboxylate derivatives

methyl 2-((1H-benzo[d]imidazol-2-yl)methylthio)-4-(4-chlorophenyl)-1,2,3,4-tetrahydro-6-methylpyrimidine-5-carboxylate(B6)

Elemental analysis (*calc.*): C, 58.80; H, 4.93; Cl, 8.27; N, 13.06; O, 7.46; S, 7.48. ¹H NMR (CHCl₃-*d*₆400 MHz) δ ppm: 1.71 (s, methyl protons of pyrimidine), 2.0 (s, N-H of pyrimidine), 3.70 (s, methyl protons of phenyl ring), 3.76 (s, methoxy protons of acetate), 4.59, 4.80 (d, methylene protons of pyrimidine), 7.00, 7.15 (s, phenyl protons), 7.26, 7.70 (s, methylene protons of diazole). ¹³C NMR (CHCl₃-*d*₆400 MHz) δ ppm: 15.2, 26.3, 58.1, 74.0, 106.0, 115.3, 123, 128.129, 132.582, 138.901, 141.5, 153.291, 167.002. MS: m/z 428.11, 429.10 (m+1), 431.10 (m+2).

methyl 2-((1H-benzo[d]imidazol-2-yl)methylthio)-1,2,3,4-tetrahydro-6-methyl-4-p-tolylpyrimidine-5-carboxylate (**B7**)

Elemental analysis (*calc.*): C, 64.68; H, 5.92; N, 13.71; O, 7.83; S, 7.85. ¹H NMR (CHCl₃-*d*₆400 MHz) δ ppm: 1.71 (s, methyl protons of pyrimidine), 2.0 (s, N-H of pyrimidine), 3.76 (s, methoxy protons of acetate), 4.59, 4.80 (d, methylene protons of pyrimidine), 6.94 (s, phenyl protons), 7.70, 7.26, 7.70 (m, aromatic protons of benzimidazole). ¹³C NMR (CHCl₃-*d*₆400 MHz) δ ppm: 15.2, 24.3, 26.3, 52.3, 58.1, 74.0, 106.0, 127.9, 128.9, 135.0, 136.7, 138.9, 141.5, 153.9, 167.2 MS: m/z 408.16, 409.17 (m+1), 410.17 (m+2).

methyl 2-((1H-benzo[d]imidazol-2-yl)methylthio)-1,2,3,4-tetrahydro-6-methyl-4-(naphthalen-1-yl)pyrimidine-5-carboxylate (**B16**)

Elemental analysis (*calc.*): C, 66.80; H, 5.37; N, 12.98; O, 7.42; S, 7.43. ¹H NMR (CHCl₃-*d*₆400 MHz) δ ppm: 1.71 (s, methyl protons of pyrimidine), 2.0 (s, N-H of pyrimidine), 3.76 (s, methoxy protons of acetate), 4.59, 4.80 (d, methylene protons of pyrimidine), 6.991 (s, phenyl protons), 7.392 (s, phenyl protons), 7.26, 7.70 (s, methylene protons of diazole) 7.32, 7.67 (m-naphthalene). ¹³C NMR (CHCl₃-*d*₆400 MHz) δ ppm: 15.2, 26.3, 56.4, 74.0, 106.0, 115.3, 124.2, 125.6, 128.6, 138.9, 141.5, 153.9 MS: m/z 431.15, 432.15 (m+1), 433.16 (m+2).

Methyl 2-((1H-benzo[d]imidazol-2-yl)methylthio)-4-(4-(trifluoromethyl)phenyl)-1,2,3,4-tetrahydro-6-methylpyrimidine-5-carboxylate (**B20**)

Elemental analysis (*calc.*): C, 57.13; H, 4.58; N, 12.11; O, 6.92; S, 6.93. ¹H NMR (CHCl₃-*d*₆400 MHz) δ ppm: 1.71 (s, methyl protons of pyrimidine), 2.0 (s, N-H of pyrimidine), 3.76 (s, methoxy protons of acetate), 4.59, 4.80 (d, methylene protons of pyrimidine), 6.99, 7.33 (s, phenyl protons), 7.392 (s, phenyl protons), 5.0 (s, methylene protons of diazole) 7.26, 7.70 (m-

benzene). ^{13}C NMR (CHCl_3 - d_6 400 MHz) δ ppm: 15.2, 26.3, 52.3, 58.1, 74.0, 106.0, 115.3, 123.0, 124.2, 125.6, 128.6, 138.9, 141.5, 153.9, 167.2. MS: m/z 462.13, 463.14 ($m+1$), 464.14 ($m+2$).

The physicochemical data of derivatives are tabulated in the Table 2.

Table 2. The physicochemical data of derivatives

Code	Molecular Formula	Molecular Weight	Melting Point ($^{\circ}\text{C}$)	R_f Value	Yield %	Solubility
B6	$\text{C}_{21}\text{H}_{21}\text{ClN}_4\text{O}_2\text{S}$	428.94	194-196	0.59	72	Ethanol, Methanol, DCM, Chloroform
B7	$\text{C}_{22}\text{H}_{24}\text{N}_4\text{O}_2\text{S}$	408.52	203-206	0.84	75	Ethanol, Methanol, DCM, Chloroform
B16	$\text{C}_{25}\text{H}_{24}\text{N}_4\text{O}_2\text{S}$	444.55	218-220	0.47	56	Ethanol, Methanol, DCM, Chloroform, Benzene
B17	$\text{C}_{21}\text{H}_{20}\text{N}_6\text{O}_6\text{S}$	484.49	265-267	0.68	67	Ethanol, Methanol, DCM, Chloroform, Benzene
B20	$\text{C}_{22}\text{H}_{21}\text{F}_3\text{N}_4\text{O}_2\text{S}$	462.49	283-285	0.93	73	Ethanol, Methanol, DCM, Chloroform

***In vitro* Biological Evaluation**

Various concentrations of derivatives were prepared in DMSO to assess their antibacterial and antifungal activities against standard strains using broth dilution. Bacteria were maintained, and drugs were diluted in nutrient Mueller Hinton broth. The broth was inoculated with 10^8 colony-forming units (cfu) per milliliter of test strains (Institute of Microbial Technology, Chandigarh, India) determined by turbidity. Stock solutions of synthesized derivate (2 mg/mL) were serially diluted for primary and secondary screening. The primary screen included 1000, 500, and 250 $\mu\text{g/mL}$ of synthesized derivatives, then those with activity were further screened at 200, 100, 50, 25, 12.5, and 6.250 $\mu\text{g/mL}$. A control without antibiotic was sub-cultured (before inoculation) by spreading one loopful evenly over a quarter of a plate of medium suitable for growing test organisms and incubated at 37°C overnight. The lowest concentrations of derivatives that inhibited bacterial or fungal growth were taken as minimal inhibitory concentrations (MICs). These were compared with the amount of control growth before incubation (original inoculum) to determine MIC accuracy. The standards for antibacterial activity were gentamycin, ampicillin, chloramphenicol, ciprofloxacin, and norfloxacin served, and those for antifungal activity were nystatin and griseofulvin. The antimalarial behavior was tested using plasmodium falciparum,

with quinine and chloroquine as the standards. Both experiments took place at the Microcare laboratory and Tuberculosis Research Centre [TRC] in Surat, Gujarat.

3. Results

Pharmacokinetic characteristics are critical to drug development because they enable scientists to investigate the biological impacts of possible pharmacological candidates (Khan et al., 2022). This compound's oral bioavailability was evaluated using Lipinski's rule of five and Veber's rules (Table 3). To better understand the pharmacokinetics profiles and drug-likeness properties of the proposed compounds, the ADME characteristics of all of them were examined (Table 4). Fig. 3 depicts the physicochemical domain that is ideal for oral bioavailability. The oral acute toxicity have been predicted along with LD₅₀ (mg/kg), toxicity class, hepatotoxicity, carcinogenicity, immunotoxicity, mutagenicity, and cytotoxicity (Table 5). Table 6 lists the ligand energies (kcal/mol), docking scores (kcal/mol), active amino acids, bond length (Å), and different interactions of derivatives with DHFR. Table 7 depicts the most potent compounds' 2D and 3D docking orientations. The results of antimicrobial and antifungal activities of the synthesized derivatives are tabulated in Table 8 which shows the MICs and MFCs respectively.

Table 3. Lipinski rule of 5 and Veber's rule calculated for methyl 2-(1*H*-pyrazol-4-ylthio)-1,2,3,4-tetrahydro-6-methylpyrimidine-5-carboxylate derivatives

Compound Codes	Lipinski rule of five					Veber's rule	
	Log P	Mol. Wt.	HBA	HBD	Violations	Total polar surface area (Å ²)	No. of rotatable bonds
NL	0.70	443.45	7	6	2	187.50	10
B1	1.62	318.39	4	3	0	104.34	5
B2	2.81	394.49	4	3	0	104.34	6
B3	0.5	440.5	6	4	0	154	7
B4	3.45	473.39	4	3	0	104.34	6
B5	3.15	412.48	5	3	0	104.34	6
B6	3.38	428.94	4	3	0	104.34	6
B7	3.12	408.52	4	3	0	104.34	6
B8	2.8	424.52	5	3	0	113.57	7
B9	2.38	410.49	5	4	0	124.57	6
B10	0.58	440.5	6	4	0	154	7
B11	2.4	410.49	5	4	0	124.57	6
B12	1.76	442.49	7	6	1	165.03	6
B13	2.44	440.52	6	4	0	133.8	7
B14	2.78	424.52	5	3	0	113.57	7
B15	3.32	420.53	4	3	0	104.34	7
B16	3.74	444.55	4	3	0	104.34	6

B17	-2.19	486.5	8	5	1	203.66	8
B18	2.51	472.58	6	3	0	146.86	7
B19	2.86	437.56	4	3	0	107.58	7
B20	3.86	462.49	7	3	0	104.34	7

Where: NL, native ligand; Mol. Wt., molecular weight; HBA, hydrogen bond acceptors; HBD, hydrogen bond donors

Table 4. The pharmacokinetics and drug-likeness properties of developed compounds

Compo und codes	Pharmacokinetics									Drug-likeness			
	GI abs.	BBB pen.	P-gp sub.	CYP1A2	CYP2C19	CYP2C9	CYP2D6	CYP3A4	Log K_p (skin permeation, cm/s)	Ghose	Egan	Muegge	Bioavailability Score
				inhibitors									
NL	L	N	Y	N	N	N	N	N	-8.81	Y	N	N	0.11
B1	High	No	Yes	No	No	No	No	No	-6.91	0	0	0	0.55
B2	High	No	Yes	No	Yes	Yes	Yes	Yes	-6.17	0	0	0	0.55
B3	Low	No	Yes	No	Yes	No	No	No	-6.91	0	1	1	0.55
B4	High	No	Yes	Yes	Yes	Yes	Yes	Yes	-6.16	0	0	0	0.55
B5	High	No	Yes	No	Yes	Yes	Yes	Yes	-6.21	0	0	0	0.55
B6	High	No	Yes	No	Yes	Yes	Yes	Yes	-5.94	0	0	0	0.55
B7	High	No	Yes	No	Yes	Yes	Yes	Yes	-6	0	0	0	0.55
B8	High	No	Yes	No	Yes	Yes	Yes	Yes	-6.38	0	0	0	0.55
B9	High	No	Yes	No	Yes	Yes	Yes	Yes	-6.52	0	0	0	0.55
B10	Low	No	Yes	No	Yes	No	No	No	-6.91	0	1	1	0.55
B11	High	No	Yes	No	Yes	Yes	Yes	Yes	-6.52	0	0	0	0.55
B12	Low	No	Yes	No	No	No	No	No	-7.22	0	1	2	0.55
B13	High	No	Yes	No	Yes	Yes	Yes	Yes	-6.73	0	1	0	0.55
B14	High	No	Yes	No	Yes	Yes	Yes	Yes	-6.38	0	0	0	0.55
B15	High	No	Yes	No	Yes	Yes	Yes	Yes	-5.88	0	0	0	0.55
B16	High	No	Yes	No	Yes	Yes	Yes	Yes	-5.59	1	0	0	0.55
B17	Low	No	Yes	No	No	No	No	No	-7.63	2	1	1	0.55
B18	Low	No	Yes	No	No	Yes	No	Yes	-7.19	1	1	0	0.55
B19	High	No	Yes	No	Yes	Yes	Yes	Yes	-6.35	1	0	0	0.55
B20	High	No	Yes	No	Yes	Yes	Yes	Yes	-5.96	0	0	0	0.55

Where: NL, Native ligand; GI abs., gastrointestinal absorption; BBB pen., blood brain barrier penetration; P-gp sub., p-glycoprotein substrate

Table 5. The predicted acute toxicities of the designed methyl 2-(1*H*-pyrazol-4-ylthio)-1,2,3,4-tetrahydro-6-methylpyrimidine-5-carboxylate derivatives

Compound codes	Parameters							
	LD ₅₀ (mg/kg)	Toxicity class	Prediction accuracy (%)	Hepatotoxicity (Probability)	Carcinogenicity (Probability)	Immunotoxicity (Probability)	Mutagenicity (Probability)	Cytotoxicity (Probability)
NL	135	3	67.38	I (0.87)	I (0.51)	I (0.99)	I (0.75)	I (0.63)
B1	1353	4	23	I (0.63)	I (0.50)	I (0.79)	I (0.56)	I (0.61)
B2	800	4	54.26	A (0.57)	A (0.50)	I (0.97)	I (0.59)	I (0.64)
B3	1000	4	54.26	A (0.54)	A (0.51)	I (0.90)	I (0.59)	I (0.65)
B4	800	4	54.26	A (0.57)	A (0.50)	I (0.85)	I (0.63)	I (0.61)
B5	800	4	54.26	A (0.56)	I (0.50)	I (0.83)	I (0.63)	I (0.64)
B6	800	4	54.26	A (0.56)	A (0.50)	I (0.90)	I (0.64)	I (0.65)
B7	800	4	54.26	A (0.56)	A (0.51)	I (0.98)	I (0.58)	I (0.66)
B8	800	4	54.26	A (0.57)	A (0.54)	I (0.84)	I (0.52)	I (0.70)
B9	800	4	54.26	A (0.58)	A (0.52)	I (0.94)	I (0.54)	I (0.69)
B10	1000	4	54.26	A (0.58)	A (0.52)	I (0.94)	I (0.54)	I (0.69)
B11	800	4	54.26	A (0.58)	A (0.52)	I (0.76)	I (0.54)	I (0.69)
B12	3000	5	54.26	A (0.58)	I (0.50)	I (0.54)	I (0.51)	I (0.69)
B13	3000	5	54.26	A (0.55)	A (0.52)	A (0.74)	I (0.53)	I (0.70)
B14	3000	5	54.26	A (0.57)	A (0.54)	I (0.62)	I (0.52)	I (0.71)
B15	1000	4	23	A (0.54)	A (0.51)	I (0.90)	I (0.59)	I (0.65)
B16	800	4	54.26	A (0.57)	A (0.50)	I (0.79)	I (0.59)	I (0.64)
B17	50	2	54.26	A (0.54)	A (0.51)	I (0.90)	I (0.59)	I (0.65)
B18	800	4	23	A (0.51)	I (0.56)	I (0.86)	I (0.63)	I (0.64)
B19	1700	4	54.26	A (0.50)	A (0.51)	I (0.79)	I (0.57)	I (0.58)
B20	1000	4	54.26	A (0.55)	I (0.50)	I (0.91)	I (0.61)	I (0.65)

Where: NL, Native ligand; I, Inactive; A, Active

Table 6. The ligand energies (kcal/mol), docking scores (kcal/mol), active amino acids, bond length (Å), and different interactions of derivatives with DHFR

Interactive amino acid residues	Bond length (Å)	Bond type	Bond category	Ligand energy	Docking score
				(kcal/mol)	
Native ligand					
ASP27	1.88237	Hydrogen bond	Conventional hydrogen bond	209.71	-8.5
ASP27	2.19462				
ALA6	3.00495				
ILE5	1.91594				
ARG57	1.96549				
ARG57	2.17225				
ILE94	3.19208	Hydrophobic	Carbon hydrogen bond		
ILE50	3.71343		Pi-Sigma		
PHE31	5.0747		Pi-Pi T-shaped		

PHE31	4.82737				
ILE94	4.98884		Alkyl		
ILE5	5.06209		Pi-Alkyl		
ALA7	4.05078				
B1					
SER49	3.68862	Hydrogen Bond	Carbon Hydrogen Bond	472.34	-7.3
MET20	5.63118	Other	Pi-Sulfur		
PHE31	4.73125	Hydrophobic	Pi-Pi T-shaped		
PHE31	4.95867				
ALA7	4.23818		Alkyl		
LEU28	5.23543		Pi-Alkyl		
ILE50	5.12738				
PHE31	5.0713				
B2					
ALA7	3.55066	Hydrogen Bond	Carbon Hydrogen Bond	592.71	-8.8
LEU28	3.91408	Hydrophobic	Pi-Sigma		
LEU28	3.85517				
ILE50	5.40423		Alkyl		
MET20	4.9061		Pi-Alkyl		
LEU28	5.15988				
MET20	5.39888				
ILE5	5.28389				
ALA7	4.43858				
B3					
GLU17	5.46623	Electrostatic	Attractive Charge	607.12	-8.5
ASP27	2.55787	Hydrogen Bond	Conventional Hydrogen Bond		
TRP30	3.48747		Carbon Hydrogen Bond		
LEU28	3.93361	Hydrophobic	Pi-Sigma		
LEU28	4.5066		Pi-Alkyl		
ALA7	4.19308				
B4					
TRP22	2.29725	Hydrogen bond	Conventional hydrogen bond	493.25	-8.2
MET20	2.61225				
TRP22	2.837				
GLU17	3.7728		Carbon hydrogen bond		

ASP27	3.90453	Electrostatic	Pi-anion		
TRP22	3.15968	Hydrogen bond	Pi-donor hydrogen bond		
PHE31	4.79282	Hydrophobic	Pi-Pi T-shaped		
ILE5	4.33985		Alkyl		
ALA7	4.22771		Pi-alkyl		
TRP30	4.75628				
PHE31	5.23494				
B5					
ASP27	5.30051	Electrostatic	Attractive Charge	590.48	-8.3
ILE94	3.0431	Hydrogen Bond	Conventional Hydrogen Bond		
SER49	3.51335		Carbon Hydrogen Bond		
GLU17	3.37871	Halogen	Halogen (Fluorine)		
MET20	5.03563	Other	Pi-Sulfur		
TYR100	5.14506	Hydrophobic	Pi-Pi T-shaped		
ALA6	5.17537		Pi-Alkyl		
ALA7	5.46509				
ILE14	4.9241				
LEU28	5.40578				
B6					
ALA7	3.52878	Hydrogen Bond	Carbon Hydrogen Bond	589.08	-9.2
LEU28	3.86687	Hydrophobic	Pi-Sigma		
LEU28	3.85918		Pi-Pi T-shaped		
PHE31	4.55541				
ILE50	5.48036				
ILE5	4.53345		Alkyl		
ALA7	4.27977				
MET20	4.94214				
LEU28	5.09768				
MET20	5.46544				
ILE5	5.28239				
ALA7	4.47741				
TRP30	5.05945				
B7					
ALA7	3.5347	Hydrogen Bond	Carbon Hydrogen Bond	589.85	-9.5
LEU28	3.89621	Hydrophobic	Pi-Sigma		

LEU28	3.85936					
ILE50	5.42506		Alkyl			
ILE5	4.51464					
ALA7	4.27187					
MET20	4.9429		Pi-Alkyl			
LEU28	5.12283					
MET20	5.42445					
ILE5	5.26046					
ALA7	4.51004					
TRP30	5.22402					
B8						
PHE31	4.03738	Other	Pi-Sulfur	532.84	-8.4	
LEU28	4.58847	Hydrophobic	Alkyl			
LYS32	4.42368		Pi-Alkyl			
ILE14	4.99272					
LEU28	4.51463					
LYS32	5.03957					
B9						
ASP27	2.7913	Hydrogen Bond	Conventional Hydrogen Bond	592.07	-9	
ASP27	2.95519		Carbon Hydrogen Bond			
ALA7	3.44573					
LEU28	3.99822	Hydrophobic	Pi-Sigma			
LEU28	3.89037		Pi-Pi T-shaped			
PHE31	4.75532					
ILE50	5.2433					Alkyl
MET20	4.97035					Pi-Alkyl
LEU28	5.21102					
MET20	5.31359					
ALA7	4.21638					
B10						
ILE94	2.76835	Hydrogen Bond	Conventional Hydrogen Bond	649.13	-8.7	
LEU24	2.33305		Carbon Hydrogen Bond			
TRP22	3.59187					
:ASN23	3.34627					
PHE31	3.99131	Hydrophobic	Pi-Sigma			
TYR100	5.50853		Pi-Pi T-shaped			
TYR100	5.0802					
ALA7	4.31723					Alkyl

ALA6	4.85734		Pi-Alkyl		
ALA7	5.44584				
ILE14	4.76935				
MET20	4.45107				
LEU28	5.1886				
B11					
THR46	2.35128	Hydrogen Bond	Conventional Hydrogen Bond	828.32	-9
ASP27	3.52188		Carbon Hydrogen Bond		
GLY96	3.34254				
MET20	3.98644	Hydrophobic	Pi-Sigma		
LEU28	3.52061				
MET20	4.41116		Alkyl		
MET20	4.84997		Pi-Alkyl		
LEU28	4.87339				
ILE14	5.42295				
B12					
TRP22	2.59159	Hydrogen Bond	Conventional Hydrogen Bond	505.71	-8.1
ASN23	2.48907				
	2.31949				
TRP22	3.21684	Hydrophobic	Carbon Hydrogen Bond		
LEU28	3.78221		Pi-Sigma		
ILE5	5.32521		Pi-Alkyl		
ALA7	4.48827				
MET20	5.20566				
B13					
ASP27	4.75067	Electrostatic	Attractive Charge	652.34	-8.3
ILE94	2.54671	Hydrogen Bond	Conventional Hydrogen Bond		
TRP22	2.38444		Carbon Hydrogen Bond		
LEU24	3.65962				
TYR100	2.99987	Other	Pi-Lone Pair		
TYR100	5.49582	Hydrophobic	Pi-Pi T-shaped		
TYR100	5.06687				
LEU24:O	4.79886		Alkyl		
LEU28	3.76538		Pi-Alkyl		
ALA6	4.84802				
ALA7	5.4843				
ILE14	4.75275				

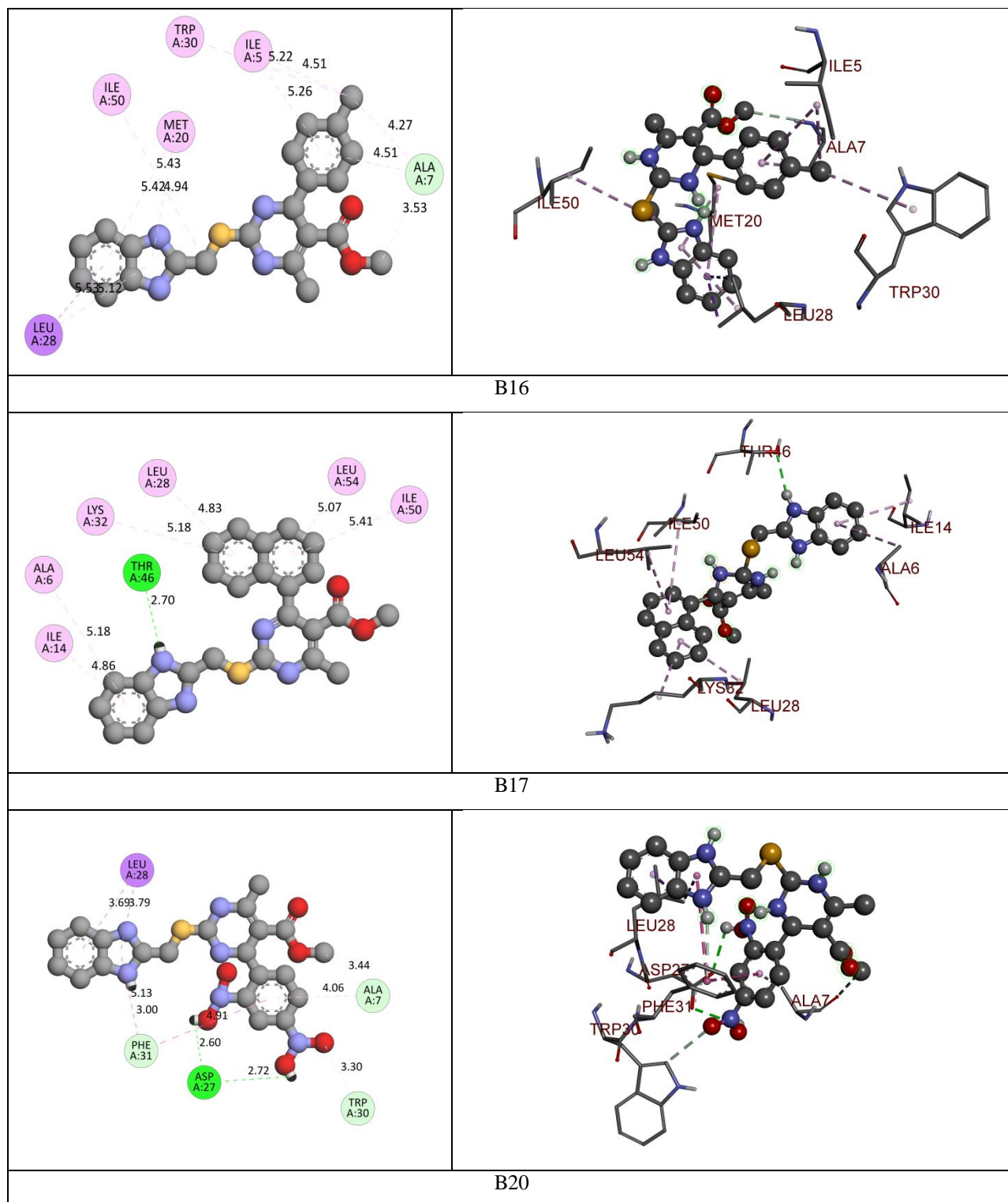
MET20	4.29044				
LEU28	5.28693				
TRP22	4.44757				
B14					
ILE94	2.56994	Hydrogen Bond	Conventional Hydrogen Bond	505.44	-7.9
PHE31	3.04666		Pi-Donor Hydrogen Bond		
MET20	4.21987	Other	Pi-Sulfur		
TYR100	5.16509	Hydrophobic	Pi-Pi T-shaped		
ILE14	4.67317		Pi-Alkyl		
LEU28	5.40769				
B15					
PRO21	2.84082	Hydrogen Bond	Conventional Hydrogen Bond	608.48	-8.6
TRP22	2.1067				
ASN23	2.30214				
GLU17	2.57783				
ILE5	5.19676	Hydrophobic	Pi-Alkyl		
ALA7	4.37387				
B16					
THR46	2.69525	Hydrogen Bond	Conventional Hydrogen Bond	707.4	-9.2
ALA6	5.17965	Hydrophobic	Pi-Alkyl		
ILE14	4.86365				
ILE50	5.414				
LEU54	5.06954				
LEU28	4.83231				
LYS32	5.17503				
B17					
ASP27	2.72473	Hydrogen Bond	Conventional Hydrogen Bond	584.86	-9.4
ASP27	2.60495		Carbon Hydrogen Bond		
ALA7	3.43784				
TRP30	3.29945				
PHE31	3.00177		Pi-Donor Hydrogen Bond		
LEU28	3.78984	Hydrophobic	Pi-Sigma		
LEU28	3.69426				
PHE31	4.9149		Pi-Pi T-shaped		
PHE31	5.13006				
ALA7	4.06114		Pi-Alkyl		

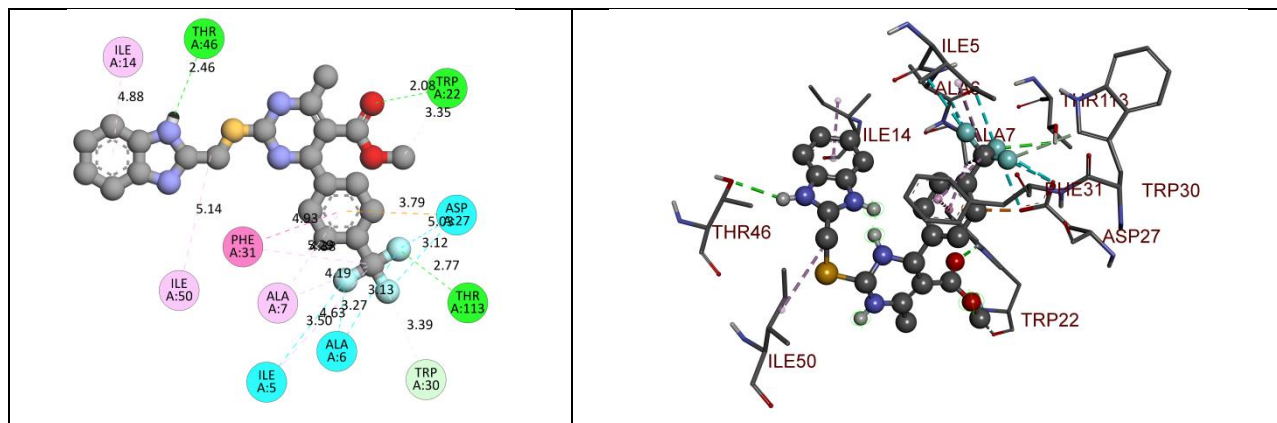
B18					
THR46	2.77726	Hydrogen Bond	Conventional Hydrogen Bond	941.05	-8.4
PHE31	2.79359		Pi-Donor Hydrogen Bond		
ILE50	5.2736	Hydrophobic	Alkyl		
ILE94	4.8951		Alkyl		
ALA6	5.23637		Pi-Alkyl		
ILE14	4.95735		Pi-Alkyl		
MET20	5.32683		Pi-Alkyl		
LEU28	5.18734		Pi-Alkyl		
B19					
ASP27	5.33901	Electrostatic	Attractive Charge	617.87	-8.1
ILE94	3.09223	Hydrogen Bond	Conventional Hydrogen Bond		
MET20	3.54195		Carbon Hydrogen Bond		
TRP22	3.42017				
ASN23	3.49954				
MET20	5.22381	Other	Pi-Sulfur		
TYR100	5.13381	Hydrophobic	Pi-Pi T-shaped		
ALA6	5.10252		Pi-Alkyl		
ALA7	5.4014				
ILE14	4.88845				
LEU28	5.30032				
B20					
THR46	2.45862	Hydrogen Bond	Conventional Hydrogen Bond	602.21	-9.6
TRP22	2.08346				
THR113	2.76505				
TRP22	3.35012		Carbon Hydrogen Bond		
TRP30	3.38747				
ILE5	3.50455	Halogen	Halogen (Fluorine)		
ALA6	3.27312				
ALA6	3.13117				
ASP27	3.01818				
ASP27	3.12254				
ASP27	3.22572				
ASP27	3.7871		Electrostatic		
PHE31	4.926	Hydrophobic	Pi-Pi T-shaped		
ILE50	5.1356		Alkyl		
ILE5	4.62669				

ALA7	4.18716		Pi-Alkyl		
ILE14	4.87638				
ALA7	4.38343				
PHE31	5.29131				

Table 7. The 2D- and 3D binding orientations of native ligand and molecules selected for the synthesis from virtual screening

2D-binding orientations	3D-binding orientations
Native ligand	
B6	
B7	



**Table 8.** The antimicrobial and antifungal activities of the synthesized derivatives

Compound code	Antimicrobial activity [MIC (μg/mL)]				Antifungal activity [MFC (μg/mL)]		
	<i>E.C.</i>	<i>P.A.</i>	<i>S.A.</i>	<i>S.P.</i>	<i>C.A.</i>	<i>A.N.</i>	<i>A.C.</i>
B6	25	25	25	50	100	100	100
B7	50	50	50	50	100	100	100
B16	25	50	50	25	100	200	100
B20	25	25	25	25	200	100	100
Gentamycin	0.05	1	0.25	0.5	NA	NA	NA
Ampicillin	100	NA	250	100	NA	NA	NA
Chloramphenicol	50	50	50	50	NA	NA	NA
Ciprofloxacin	25	25	50	50	NA	NA	NA
Norfloxacin	10	10	10	10	NA	NA	NA
Nystatin	NA	NA	NA	NA	100	100	100
Greseofulvin	NA	NA	NA	NA	500	100	100

Where,

E.C., *Escherichia coli*; *P.A.*, *Pseudomonas aeruginosa*; *S.A.*, *Staphylococcus aureus*; *S.P.*, *Staphylococcus pyogenes*; *C.A.*, *Candida albicans*; *A.N.*, *Aspergillus niger*; *A.C.*, *Aspergillus clavatus*; *MIC*, Minimum inhibitory concentration; *MFCs*, minimum fungicidal concentration.

4. Discussion

In present study we have designed and developed some methyl 2-(1*H*-pyrazol-4-ylthio)-1,2,3,4-tetrahydro-6-methylpyrimidine-5-carboxylate derivatives as potential DHFR inhibitors. In accordance with Lipinski's and Veber's rule (Table 2), few molecules have violated both the rules. The log P values of all the molecules were found to be between -0.15 to 2.61 which indicate optimum lipophilicity. Lipophilicity is a significant feature of the molecule that affects how it works in the body (S. Khan et al., 2021). It is determined by the compound's Log P value, which

measures the drug's permeability in the body to reach the target tissue (Krzywinski and Altman, 2013; Lipinski et al., 2012). The molecular weight of all the molecules was below 500 Da which indicates active better transport of the molecules through biological membrane. Fortunately, the Lipinski rule of 5 had not been compromised by the compounds, excluding native ligand and compounds **B12**, **B17**, which displayed 2 and 1 violations of Lipinski rule respectively (Khan et al., 2022; Shntaif et al., 2021). The total polar surface area (TPSA) and the number of rotatable bonds have been found to better discriminate between compounds that are orally active or not. According to Veber's rule, TPSA should be ≤ 140 and number of rotatable bonds should be ≤ 10 . It was observed that native ligand violated the Veber's rule, as it has TPSA 187.50 \AA^2 and number of rotatable bonds 10 which indicate its poor oral bioavailability. Molecules **B6**, **B7**, **B16** and **B20** have showed more TPSA than acceptable value therefore these compounds were indicated poor oral bioavailability.

In order to further optimize the compounds, pharmacokinetics and drug-likeness properties were calculated for each one. All the compounds including native ligand showed no penetration to the blood-brain barrier (BBB). The $\log K_p$ (skin penetration, cm/s) and bioavailability values of all the compounds were within acceptable limits. Few molecules and native ligand do not meet all, two, or one of the Ghose, Egan, and Muegge requirements (Table 3). Molecules **B3**, **B10**, **B12**, **B18**, and native ligand exhibited low gastrointestinal (GI) absorption.

In acute toxicity predictions, one molecule i.e. **B17** falls in toxicity class-II [fatal if swallowed ($5 < LD_{50} \leq 50$)] whereas, native ligand fall in toxicity class-III i.e. toxic if swallowed ($50 < LD_{50} \leq 300$). All Molecules except **B12**, **B13**, and **B14** displayed toxicity class-IV which means harmful if swallowed ($300 < LD_{50} \leq 2000$). Molecules **B12**, **B13**, and **B14** showed toxicity class-V which indicate may be harmful if swallowed ($2000 < LD_{50} \leq 5000$) (Banerjee et al., 2018). From this virtual screening, it was concluded that compounds **B6**, **B7**, **B16**, and **B20** do possess drug-like properties and hence were subjected to molecular docking studies.

The binding affinities of the derivatives have been compared with the binding mode of native ligand present in the crystal structure of DHFR (PDB ID: 5CCC). Native ligand exhibited -

8.5 kcal/mol of binding affinity with DHFR and formed 6 conventional hydrogen bonds with Asp27, Ala6, Ile5, Arg57, and one carbon-hydrogen bond with Ile94. It has developed many hydrophobic interactions such as Pi-sigma, Pi-Pi T-shaped, alkyl, and Pi-alkyl bonds with Ile50, Phe31, Ile94, Ile5, and Ala7.

Compound **B6** exhibited -9.2 kcal/mol binding affinity and formed one carbon hydrogen bond with Ala7. It displayed many hydrophobic interactions (Pi-Sigma, Pi-Pi T-shaped alkyl and Pi-alkyl,) with Leu28, Phe31, Ile50, Ala7, Met20, Trp30. Compound **B7** displayed -9.5 kcal/mol docking score and formed only one carbon hydrogen bond Ala7. It displayed many hydrophobic interactions (Pi-Sigma, alkyl and Pi-alkyl) with Leu28, Ile50, Ala7, Met20, and Trp30. Compound **B16** showed -9.2 kcal/mol binding affinity and developed one conventional hydrogen bond with Thr46. It also formed pi-alkyl type of hydrophobic Interactions with Ala6, Ile14, Ile 50, Leu54, Leu28, and Lys32. Compound **B20** exhibited -9.2 kcal/mol of binding affinity and developed three conventional hydrogen bonds with Thr46, Trp22 & Thr113, whereas formed two carbon hydrogen bonds with Trp22 and Ile5. It also formed pi-alkyl & alkyl type of hydrophobic Interactions with Ala7, Ile14, Ile 50 and Phe31, Electrostatic Interactions with Asp27 and Phe31.

Millions of humans are now affected by bacterial diseases triggered by pathogenic bacteria which are responsible for elevated child mortality rates in developed countries ^[9]. Not all bacteria are pathogenic. For example, there are thousands of bacterial organisms in the human digestive tract, some of which are harmless and even useful. Furthermore, various mechanisms of action on the target site can aid in the discovery of potential drugs while developing antibacterial agents ^[10]. However, since bacteria have developed antibiotic tolerance, finding a new antibacterial agent became difficult. Gram-positive bacteria, such as *methicillin-resistant S. aureus*, *S. epidermis*, *vancomycin-resistant E. calcium*, and *penicillin-resistant S. pneumoniae*, induce the majority of bacterial infections. Fungal infections have become more frequent, and the majority of them are minor (Manohar et al., 2020). There are various varieties of fungi that cause infections today (Reta et al., 2019). Species like *candida* and *aspergillus* are only a few examples (Liu et al., 2017). In present investigation, all the synthesized compounds were subjected for *in vitro* antibacterial and antifungal activity using different strains as given in Table 7.

All the synthesized compounds were sensitive to both gram +ve(*Staphylococcus aureus*, *Staphylococcus pyogenes*) and gram –ve(*Escherichia coli*, *Pseudomonas aeruginosa*) bacterial strains. All the compounds demonstrated more potent activity than Ampicillin against both gram-positive and gram-negative bacteria. Most of the compounds were more or equipotent than Chloramphenicol and Ciprofloxacin. Compound **B16** was sensitive at 25 µg/mL against *Escherichia coli*, 50 µg/mL against *Pseudomonas aeruginosa*, and *Staphylococcus aureus* whereas compound **B20** was sensitive to all gram +ve and –ve bacteria at same concentration. Compound **B6** was sensitive at 50 µg/mL against all the bacteria. In antifungal activity, compound **B7** exhibited MFCs of 100 µg/mL against *Candida albicans*, *Aspergillus niger*, and *Aspergillus clavatus* which is same as Nystatin. Compound **B16** and **B20** were also sensitive to all the antifungal strains at 100 or 200 µg/mL concentration. Compound **B20** is more potent than Greseofulvin against *Candida albicans*. It can be concluded that substitution at para-position with bulky group can greatly increase the activity of the designed compounds.

5. Conclusion

Dihydrofolate reductase (DHFR) is an important enzyme required to maintain bacterial growth, and hence inhibitors of DHFR have been proven as effective agents for treating bacterial infections. In the present study, we have designed and developed some methyl 2-(1*H*-pyrazol-4-ylthio)-1,2,3,4-tetrahydro-6-methylpyrimidine-5-carboxylate derivatives as potential DHFR inhibitors. The designed derivatives were screened through Lipinski rule, Veber's rule, ADMET analysis, drug-likeness properties, and molecular docking. The selected derivatives were synthesized and subjected for *in vitro* biological evaluation. We concluded that compounds **B6**, **B7**, **B16**, and **B20** are most potent and can be developed further to get more promising molecules for the treatment of bacterial infection.

References

- Ahmed Elkanzi, N.A., 2020. Synthesis and Biological Activities of Some Pyrimidine Derivatives: A Review. Orient. J. Chem. 36, 1001–1015. <https://doi.org/10.13005/ojc/360602>
- Anwar, K., Hussein, D., Salih, J., 2020. Antimicrobial susceptibility testing and phenotypic detection of MRSA isolated from diabetic foot infection. Int. J. Gen. Med. 13, 1349–1357.

<https://doi.org/10.2147/IJGM.S278574>

- Banerjee, P., Eckert, A.O., Schrey, A.K., Preissner, R., 2018. ProTox-II: A webserver for the prediction of toxicity of chemicals. *Nucleic Acids Res.* 46, W257–W263. <https://doi.org/10.1093/nar/gky318>
- Bhat, A.R., Dongre, R.S., Naikoo, G.A., Hassan, I.U., Ara, T., 2017. Proficient synthesis of bioactive annulated pyrimidine derivatives: A review. *J. Taibah Univ. Sci.* 11, 1047–1069. <https://doi.org/10.1016/j.jtusci.2017.05.005>
- Chaudhari, R.N., Khan, S.L., Chaudhary, R.S., Jain, S.P., Siddiqui, F.A., 2020. B-Sitosterol: Isolation from *Muntingia Calabura* Linn Bark Extract, Structural Elucidation And Molecular Docking Studies As Potential Inhibitor of SARS-CoV-2 Mpro (COVID-19). *Asian J. Pharm. Clin. Res.* 13, 204–209. <https://doi.org/10.22159/ajpcr.2020.v13i5.37909>
- Daina, A., Michielin, O., Zoete, V., 2017. SwissADME: A free web tool to evaluate pharmacokinetics, drug-likeness and medicinal chemistry friendliness of small molecules. *Sci. Rep.* 7. <https://doi.org/10.1038/srep42717>
- Dallakyan, S., Olson, A.J., 2015. Small-molecule library screening by docking with PyRx. *Methods Mol. Biol.* 1263, 243–250. https://doi.org/10.1007/978-1-4939-2269-7_19
- Durga devi, D., Manivarman, S., Subashchandrabose, S., 2017. Synthesis, molecular characterization of pyrimidine derivative: A combined experimental and theoretical investigation. *Karbala Int. J. Mod. Sci.* 3, 18–28. <https://doi.org/10.1016/j.kijoms.2017.01.001>
- He, J., Qiao, W., An, Q., Yang, T., Luo, Y., 2020. Dihydrofolate reductase inhibitors for use as antimicrobial agents. *Eur. J. Med. Chem.* 195. <https://doi.org/10.1016/j.ejmech.2020.112268>
- Indora, N., Kaushik, D., 2015. Design , development and evaluation of ethosomal gel of fluconazole for topical fungal infection. *Int. J. Eng. Sci. Invent. Res. Dev.* I, 280–306.
- Jouhar, L., Jaafar, R.F., Nasreddine, R., Itani, O., Haddad, F., Rizk, N., Hoballah, J.J., 2020. Microbiological profile and antimicrobial resistance among diabetic foot infections in Lebanon. *Int. Wound J.* 17, 1764–1773. <https://doi.org/10.1111/iwj.13465>
- Khan, A., Unnisa, A., Soheli, M., Date, M., Panpaliya, N., Saboo, S.G., Siddiqui, F., Khan, S., 2022. Investigation of phytoconstituents of *Enicostemma littorale* as potential glucokinase activators through molecular docking for the treatment of type 2 diabetes mellitus. *Silico Pharmacol.* 10. <https://doi.org/10.1007/s40203-021-00116-8>
- Khan, S., Kale, M., Siddiqui, F., Nema, N., 2021. Novel pyrimidine-benzimidazole hybrids with antibacterial and antifungal properties and potential inhibition of SARS-CoV-2 main protease and spike glycoprotein. *Digit. Chinese Med.* 4, 102–119. <https://doi.org/10.1016/j.dcm.2021.06.004>

- Khan, S.L., Siddiqui, F.A., Jain, S.P., Sonwane, G.M., 2020. Discovery of Potential Inhibitors of SARS-CoV-2 (COVID-19) Main Protease (Mpro) from Nigella Sativa (Black Seed) by Molecular Docking Study. *Coronaviruses* 2, 384–402. <https://doi.org/10.2174/2666796701999200921094103>
- Khan, S.L., Siddiqui, F.A., Shaikh, M.S., Nema, N. V., Shaikh, A.A., 2021. Discovery of potential inhibitors of the receptor-binding domain (RBD) of pandemic disease-causing SARS-CoV-2 Spike Glycoprotein from Triphala through molecular docking. *Curr. Chinese Chem.* 01. <https://doi.org/10.2174/2666001601666210322121802>
- Khan, Sharuk L., Sonwane, G.M., Siddiqui, F.A., Jain, S.P., Kale, M.A., Borkar, V.S., 2020. Discovery of Naturally Occurring Flavonoids as Human Cytochrome P450 (CYP3A4) Inhibitors with the Aid of Computational Chemistry. *Indo Glob. J. Pharm. Sci.* 10, 58–69. <https://doi.org/10.35652/igjps.2020.10409>
- Kim, S., Chen, J., Cheng, T., Gindulyte, A., He, J., He, S., Li, Q., Shoemaker, B.A., Thiessen, P.A., Yu, B., Zaslavsky, L., Zhang, J., Bolton, E.E., 2021. PubChem in 2021: New data content and improved web interfaces. *Nucleic Acids Res.* 49, D1388–D1395. <https://doi.org/10.1093/nar/gkaa971>
- Krzywinski, M., Altman, N., 2013. Points of significance: Significance, P values and t-tests. *Nat. Methods* 10, 1041–1042. <https://doi.org/10.1038/nmeth.2698>
- Lipinski, C.A., Lombardo, F., Dominy, B.W., Feeney, P.J., 2012. Experimental and computational approaches to estimate solubility and permeability in drug discovery and development settings. *Adv. Drug Deliv. Rev.* <https://doi.org/10.1016/j.addr.2012.09.019>
- Liu, Q., Meng, X., Li, Y., Zhao, C.N., Tang, G.Y., Li, H. Bin, 2017. Antibacterial and antifungal activities of spices. *Int. J. Mol. Sci.* 18. <https://doi.org/10.3390/ijms18061283>
- Loi, V. Van, Huyen, N.T.T., Busche, T., Tung, Q.N., Gruhlke, M.C.H., Kalinowski, J., Bernhardt, J., Slusarenko, A.J., Antelmann, H., 2019. Staphylococcus aureus responds to allicin by global S-thioallylation – Role of the Brx/BSH/YpdA pathway and the disulfide reductase MerA to overcome allicin stress. *Free Radic. Biol. Med.* 139, 55–69. <https://doi.org/10.1016/j.freeradbiomed.2019.05.018>
- Manohar, P., Loh, B., Athira, S., Nachimuthu, R., Hua, X., Welburn, S.C., Leptihn, S., 2020. Secondary Bacterial Infections During Pulmonary Viral Disease: Phage Therapeutics as Alternatives to Antibiotics? *Front. Microbiol.* 11. <https://doi.org/10.3389/fmicb.2020.01434>
- Marchese, A., Barbieri, R., Sanches-Silva, A., Daglia, M., Nabavi, S.F., Jafari, N.J., Izadi, M., Ajami, M., Nabavi, S.M., 2016. Antifungal and antibacterial activities of allicin: A review. *Trends Food Sci. Technol.* 52, 49–56. <https://doi.org/10.1016/j.tifs.2016.03.010>

- Mittersteiner, M., Farias, F.F.S., Bonacorso, H.G., Martins, M.A.P., Zanatta, N., 2021. Ultrasound-assisted synthesis of pyrimidines and their fused derivatives: A review. *Ultrason. Sonochem.* 79. <https://doi.org/10.1016/j.ultsonch.2021.105683>
- Mohana Roopan, S., Sompalle, R., 2016. Synthetic chemistry of pyrimidines and fused pyrimidines: A review. *Synth. Commun.* 46, 645–672. <https://doi.org/10.1080/00397911.2016.1165254>
- Murali, T.S., Kavitha, S., Spoorthi, J., Bhat, D. V., Prasad, A.S.B., Upton, Z., Ramachandra, L., Acharya, R. V., Satyamoorthy, K., 2014. Characteristics of microbial drug resistance and its correlates in chronic diabetic foot ulcer infections. *J. Med. Microbiol.* 63, 1377–1385. <https://doi.org/10.1099/jmm.0.076034-0>
- Nerkar, A.U., 2021. Use of Pyrimidine and Its Derivative in Pharmaceuticals: A Review. *J. Adv. Chem. Sci.* 7, 729–732. <https://doi.org/10.30799/jacs.239.21070203>
- Qin, H.L., Zhang, Z.W., Lekkala, R., Alsulami, H., Rakesh, K.P., 2020. Chalcone hybrids as privileged scaffolds in antimalarial drug discovery: A key review. *Eur. J. Med. Chem.* 193. <https://doi.org/10.1016/j.ejmech.2020.112215>
- Rahman, M., Hasan, M.F., Das, R., Khan, A., 2009. The Determination of Antibacterial and Antifungal Activities of Polygonum hydropiper (L.) Root Extract. *Adv. Biol. Res. (Rennes)*. 3, 53–56.
- Rappé, A.K., Casewit, C.J., Colwell, K.S., Goddard, W.A., Skiff, W.M., 1992. UFF, a Full Periodic Table Force Field for Molecular Mechanics and Molecular Dynamics Simulations. *J. Am. Chem. Soc.* 114, 10024–10035. <https://doi.org/10.1021/ja00051a040>
- Reta, A., Bitew Kifilie, A., Mengist, A., 2019. Bacterial Infections and Their Antibiotic Resistance Pattern in Ethiopia: A Systematic Review. *Adv. Prev. Med.* 2019, 1–10. <https://doi.org/10.1155/2019/4380309>
- San Diego: Accelrys Software Inc., 2012. Discovery Studio Modeling Environment, Release 3.5. Accelrys Softw. Inc.
- Sánchez-Sánchez, M., Cruz-Pulido, W.L., Bladinieres-Cámara, E., Alcalá-Durán, R., Rivera-Sánchez, G., Bocanegra-García, V., 2017. Bacterial Prevalence and Antibiotic Resistance in Clinical Isolates of Diabetic Foot Ulcers in the Northeast of Tamaulipas, Mexico. *Int. J. Low. Extrem. Wounds* 16, 129–134. <https://doi.org/10.1177/1534734617705254>
- Sanchez, E., Doron, S., 2016. Bacterial Infections: Overview, in: *International Encyclopedia of Public Health*. pp. 196–205. <https://doi.org/10.1016/B978-0-12-803678-5.00030-8>
- Shen, Z.L., Xu, X.P., Ji, S.J., 2010. Brønsted base-catalyzed one-pot three-component Biginelli-type reaction: An efficient synthesis of 4,5,6-triaryl-3,4-dihydropyrimidin-2(1H)-one and mechanistic

- study. *J. Org. Chem.* 75, 1162–1167. <https://doi.org/10.1021/jo902394y>
- Shntaif, A.H., Khan, S., Tapadiya, G., Chettupalli, A., Saboo, S., Shaikh, M.S., Siddiqui, F., Amara, R.R., 2021. Rational drug design, synthesis, and biological evaluation of novel N-(2-arylamino-phenyl)-2,3-diphenylquinoxaline-6-sulfonamides as potential antimalarial, antifungal, and antibacterial agents. *Digit. Chinese Med.* 4, 290–304. <https://doi.org/10.1016/j.dcmmed.2021.12.004>
- Siddiqui, F.A., Khan, S.L., Marathe, R.P., Nema, N. V., 2021. Design, Synthesis, and In Silico Studies of Novel N-(2-Amino-phenyl)-2,3-Diphenylquinoxaline-6-Sulfonamide Derivatives Targeting Receptor- Binding Domain (RBD) of SARS-CoV-2 Spike Glycoprotein and their Evaluation as Antimicrobial and Antimalarial Agents. *Lett. Drug Des. Discov.* 18, 915–931. <https://doi.org/10.2174/1570180818666210427095203>
- Songsunthong, W., Prasopporn, S., Bohan, L., Srimanote, P., Leartsakulpanich, U., Yongkiettrakul, S., 2021. A novel bicyclic 2,4-diaminopyrimidine inhibitor of *Streptococcus suis* dihydrofolate reductase. *PeerJ* 9. <https://doi.org/10.7717/peerj.10743>
- Verma, V., Joshi, C.P., Agarwal, A., Soni, S., Kataria, U., 2020. A Review on Pharmacological Aspects of Pyrimidine Derivatives. *J. Drug Deliv. Ther.* 10, 358–361. <https://doi.org/10.22270/jddt.v10i5.4295>
- Wróbel, A., Arciszewska, K., Maliszewski, D., Drozdowska, D., 2020. Trimethoprim and other nonclassical antifolates an excellent template for searching modifications of dihydrofolate reductase enzyme inhibitors. *J. Antibiot. (Tokyo)*. 73, 5–27. <https://doi.org/10.1038/s41429-019-0240-6>